

Accelerated Stress Tests and Statistical Reliability Analysis of Metal-Oxide/GaN Nanostructured Sensor Devices

Md Ashfaque Hossain Khan[✉], Ratan Debnath, Abhishek Motayed, and Mulpuri V. Rao, *Senior Member, IEEE*

Abstract—In this work, sensor die/process and packaging reliabilities of metal-oxide/GaN nanowire-based gas sensors have been studied for the first time, using industry standard accelerated lifetime tests, such as- High Temperature Operating Life, High Temperature Storage Life, Temperature Cycling Test and Highly Accelerated Stress Test. The metal-oxide functionalization used for sensing ethanol exposure in this study is ZnO. For all the tests, sample ZnO/GaN devices have been exposed to 500 ppm of ethanol in dry air at room temperature (20°C) to observe and record the degradation of signal to noise ratio (SNR) as a function of stress time and number of thermal cycles. Although no complete device failure was observed in any of the performed tests, gas sensing response kept decreasing gradually due to increasing stress. The lowering of the sensor response is believed to be due to gradual phase transformation of the receptor ZnO and baseline resistance increase. The method for estimating failure rate and lifetime of sensor devices has been discussed in detail. Using statistical data from the performed accelerated stress tests, chi-square distribution has been implemented to predict the failure rate and lifetime of GaN nanostructured sensor devices. The mean-time-to-failure (MTTF) of the stressed devices of this study is about 4 years.

Index Terms—Device reliability, accelerated stress, statistical analysis, sensor device, gas sensor.

I. INTRODUCTION

SEMICONDUCTOR device reliability can be defined as the ability of a device to perform its specified function for a specified time-period under specified environmental conditions. Wide band-gap semiconductors have the potential to provide environmental and radiation stability, which are useful for making reliable and robust gas sensors to operate in hostile conditions [1], [2]. Having wide bandgap (3.4 eV), Gallium Nitride (GaN) is less vulnerable to attack in caustic environments, and resistant to radiation because of the larger cohesion energies among its constituent atoms [3]. So,

Manuscript received April 18, 2020; revised August 11, 2020; accepted October 1, 2020. Date of publication October 5, 2020; date of current version December 8, 2020. This work was supported in part by NSF under Grant ECCS1840712, and in part by the Internal Funding from N5 Sensors, Inc. (Corresponding authors: Md Ashfaque Hossain Khan; Mulpuri V. Rao.)

Md Ashfaque Hossain Khan and Mulpuri V. Rao are with the Department of Electrical and Computer Engineering, George Mason University, Fairfax, VA 22030 USA (e-mail: mkhan53@gmu.edu; rmulpuri@gmu.edu).

Ratan Debnath and Abhishek Motayed are with Device Research and Development Department, N5 Sensors Inc., Rockville, MD 20850 USA.

Color versions of one or more of the figures in this article are available online at <https://ieeexplore.ieee.org>.

Digital Object Identifier 10.1109/TDMR.2020.3028786

AlGaN/GaN-based devices are expected to work in chemically harsh environments, at high temperatures and under radiation fluxes due to having thermally and chemically stable structures [4], [5].

Previously, metal oxide functionalized GaN nanowire-based devices have been fabricated and employed for high performance sensing of various toxic gases [6]–[11]. For real world applications, estimation of failure rate and operating lifetime by studying possible failure mechanisms through standard accelerated lifetime tests is an essential task which to the best of our knowledge was not reported to date for the sensor devices.

In this study, for the first time, we have investigated various accelerated lifetime tests on metal-oxide (ZnO in this work) functionalized GaN nanowire-based gas sensor devices. The impact of the applied stresses on packaging and sensor die has been thoroughly studied. In this work, all the accelerated tests have been performed following the reliability standards of Joint Electron Device Engineering Council (JDEC) [12]. The approach for estimating failure rate and lifetime of sensor device has been presented. The gas sensing data before and after applying the reliability tests have been collected continuously and analyzed by chi-square distribution to obtain the device reliability statistics.

II. METHOD FOR ESTIMATING OPERATING-LIFE FAILURE RATE

Generally, two functions are used in the evaluation of reliability of semiconductor sensor devices. They are probability density function (pdf) of failure $f(t)$ and failure rate $\lambda(t)$. The $f(t)$ denotes the probability of a device failing in the time interval dt at time t . It is related to the Cumulative Distribution Function (CDF), $F(t)$, as $f(t) = dF(t)/dt$. On the other hand, failure rate $\lambda(t)$ is defined as the instantaneous failure rate of a device having survived to time t .

The bathtub curve depicted in Figure 1 describes the relative variation of the failure rate of the entire population of sensor devices over time.

Typically, there are three different failure regions in a sensor device lifetime as illustrated in the failure rate curve. Firstly, early failure rate emerges from the wafer processing defects (crystal defects, dust) that make the device inherently defective from the start and likely to fail on applying mild environmental stress. Some devices may fail at relatively early stage due

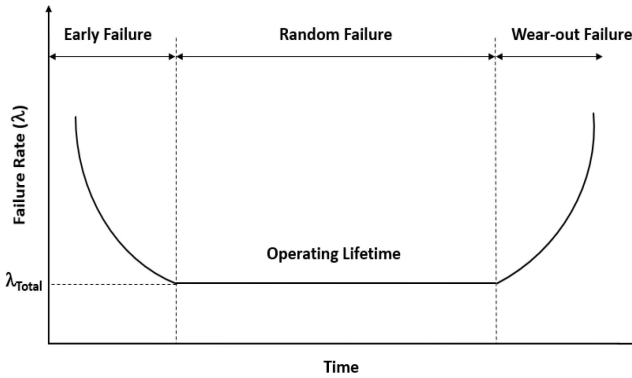


Fig. 1. The bathtub curve showing the relative variation of failure rate of the sensor devices over time.

to the presence of defects in the metal oxide material, fragile wire bond pad, processing errors etc. In order to address these early failures, a screening method called “burn-in” is carried out where a short time stress is applied before shipping to eliminate devices containing early defects [13]. Secondly, random failures occur during the useful lifetime of the device which remains almost constant over time. Most of the sensors are expected to last longer with a constant failure rate represented by the bottom of the bathtub. In this area, a failure might be caused by an operational constraint of the sensors being violated, for instance, extreme humidity and temperature conditions or voltage excursions. Also, devices may fail after a long period because of relatively insignificant early defects. Lastly, device wear-out failures arise from the durability of the constituent semiconductor materials. The increasing failure rate is mainly due to the fatigue of the metal oxide or semiconductor material or the end of the lifecycle of the LED or other components present inside the chip [14]. The wear-out failure rate increases with time until all the devices gradually fail or exhibit characteristic defects. Sensor device lifetime can be estimated by the time at which the cumulative wear-out failure rate reaches a defined threshold value. Here, the method for estimating operating life failure rate of GaN nanowire-based devices has been discussed in detail.

The operating life failure rate can be computed by dividing the number of device failures by the device operational hours, expressed as failures per billion device hours (FITs). In this case, a fraction of total sample devices is tested to obtain the failure rate. It is well known that it is necessary to make use of specific probability distribution to determine the unknown population parameter from known sample statistics [15]. The chi-square distribution (χ^2) relates observed and expected frequencies of an event, which can be employed to determine the unknown sample parameter from known sample statistics. The failure rate at stress conditions is related with the chi-square distribution by the equation given below [16]:

$$\lambda_{stress} = \frac{\chi^2(\alpha, n)}{2t} \quad (1)$$

where, λ_{stress} = failure rate at stress conditions, χ^2 = chi-square function, α = confidence level, n = degree of freedom = $2(r + 1)$, r = number of failures, and t = device-hours.

Device-hours are defined as the product of the number of devices that are stress tested and the duration of the stress test. In this work, failure limit of the sensor device has been defined as the degradation of signal to noise ratio (SNR) by more than 50% of its initial value. There is a gradual degradation in SNR of sensor devices without accelerated stresses. Also, it was observed previously that sensor output signal can be well distinguished up to a decay of half of its initial response. Therefore, SNR degradation of 50% has been set as a reasonable criterion for the sensor failure.

Here, all the device reliability tests have been performed under accelerated stress conditions. The acceleration factors of different stresses can be calculated in the following ways [17]–[20].

A. Thermal Acceleration Factor

Acceleration factor for thermal stress is calculated using the Arrhenius equation:

$$AF_t = e^{\left[\frac{E_a}{k} \left(\frac{1}{273+T_{use}} - \frac{1}{273+T_{stress}} \right) \right]} \quad (2)$$

where, AF_t = thermal acceleration factor, E_a = activation energy in electron Volts (eV) = 0.28 eV (ZnO), k = Boltzmann's constant = 8.6×10^{-5} eV/K, T_{use} = junction temperature at normal use condition in °C = 20°C (in this case), and T_{stress} = the stress temperature in °C.

B. Temperature Cycling Acceleration Factor

The acceleration factor can be estimated by:

$$AF_{tc} = \left(\frac{T_{max,stress} - T_{min,stress}}{T_{max,use} - T_{min,use}} \right)^n \quad (3)$$

where, $T_{max,stress}$ = high temperature in cycling stress, $T_{min,stress}$ = low temperature in cycling stress, $T_{max,use}$ = high temperature in field application, usually 70°C, $T_{min,use}$ = low temperature in field application, usually 0°C, n = experimentally determined exponent, usually $n = 4$ for Au, which is used here as an electric connector between device bond pad and packaging pins.

C. Voltage Acceleration Factor

The acceleration factor due to voltage stress, AF_v can be derived from Eyring model as:

$$AF_v = e^{\gamma(V_{stress} - V_{use})} \quad (4)$$

where, AF_v = voltage acceleration factor, γ = constant = 3 V^{-1} (for GaN), V_{stress} = stress voltage and V_{use} = nominal operating voltage = 5 V (in this case).

D. Humidity Acceleration Factor

For humidity acceleration test, the acceleration factor (AF_h) can be estimated by:

$$AF_h = \left(\frac{RH_{stress}}{RH_{use}} \right)^m \quad (5)$$

where, RH_{stress} = relative humidity in stress, RH_{use} = nominal working relative humidity = 30% (here) and m = experimentally determined exponent, usually $m = 3$ for Au, which is

TABLE I
THE PERFORMED ACCELERATED DEVICE RELIABILITY TESTS AND THEIR TEST CONDITION SPECIFICATIONS

Accelerated Stress Test	Test Conditions
Die/Process Reliability Tests	
High Temperature Operating Life (HTOL)	$T_{stress} = 120^{\circ}\text{C}$, $V_{stress} = 5.5\text{ V}$ (1.1x V_{bias}), 30 days Ref: JEDEC 22-A-A108
High Temperature Storage Life (HTSL)	$T_{stress} = 150^{\circ}\text{C}$, Unbiased, 2400 hrs. Ref: JESD22-A103
Package Reliability Tests	
Temperature Cycling Test (TCT)	$T_{max,stress} = 180^{\circ}\text{C}$, $T_{min,stress} = -60^{\circ}\text{C}$, 500 cycles; Duration of each cycle 25 minutes, including transition time; Ref: JEDEC 22-B-A104
Highly Accelerated Stress Test (HAST)	$T_{STRESS} = 130^{\circ}\text{C}$, 85% RH, $V_{stress} = 5.5\text{ V}$ (1.1x V_{bias}), 96 hrs.; Ref: JEDEC 22A110

used here as an electric connector between device bond pad and packaging pins.

The mean-time-to-failure (MTTF) is defined as the average time-to-failure for a population of devices operating at the required function, under the specified conditions for a stated period. It can be represented by:

$$MTTF = \int_0^{\infty} tf(t)dt \quad (6)$$

For the case of constant failure rate ($\lambda(t) = \text{constant}$), $R(t) = \exp(-\lambda t)$. $R(t)$ is the probability that a device will perform a defined function without failure under stated conditions for a stated length of time. $F(t) = 1 - \exp(-\lambda t)$ and $f(t) = dF(t)/dt = \lambda \exp(-\lambda t)$, therefore,

$$MTTF = \frac{1}{\lambda_{total}} \quad (7)$$

where the point estimate of the failure rate at operating conditions is calculated as:

$$\lambda_{total} = \frac{\lambda_{stress}}{\text{Accelerating Factors}}. \quad (8)$$

III. EXPERIMENTAL DETAILS

The ZnO functionalized GaN nanowire-based sensor devices have been fabricated using industry-standard top-down fabrication technique in a class 100 cleanroom. The nanowires were formed on silicon substrate by production standard stepper lithography assisted inductively coupled plasma (ICP) etching of GaN epilayer grown on Si substrate. A thin layer (5-10 nm) of ZnO was deposited on nanowire surface by RF magnetron sputtering followed by rapid thermal annealing (RTA). The details of the device fabrication including the process flow diagram can be found in our previous papers [21]–[25]. Finally, metal bond pads (Ti/Au) were deposited on the device die and wire bonded to leadless chip carrier (LCC) packages.

Before applying any stress condition, the current-voltage characteristics of the fabricated devices were examined by a National Instrument (NI) PXI SMU system under a LED UV light source having a wavelength of 365 nm and output power of 470 mW/cm². The working sensor devices were placed in a custom designed gas chamber made of stainless steel for ethanol sensing data collection (Figure 2). Gas bubbler was used to produce ethanol vapor from liquid ethanol.



Fig. 2. ZnO/GaN sensor chips with their data collection set-up within gas chamber.

A mixture of ethanol and compressed breathing air was flowed into the sensing chamber and the net flow (air + ethanol) was maintained at 0.5 slpm. Mass flow controllers (MFCs) independently controlled the flow rate of each component, determining the composition of the mixed gas. The sensor currents were measured by the NI PXI SMU system at a constant 5V DC voltage. Sensor responses were calculated in the form of signal to noise ratio (SNR), expressed in decibel (dB). The noise was obtained by evaluating the standard deviation of the raw sensor response.

Typically, accelerated stress tests are performed on fabricated semiconductor devices to accelerate common failure modes including parametric shifts, high leakage, catastrophic failure etc. [26]. The device reliability tests can be divided into two parts, (1) Die/Process Reliability Tests and (2) Package Reliability Tests. The accelerated device reliability tests performed here are listed in Table I with their test conditions in detail. These tests and their specifications have been chosen from JEDEC Standard, which have been universally used throughout the semiconductor industry [27]–[29].

The purpose of high temperature operating life (HTOL) test is to accelerate failure mechanisms that are activated by temperature while under bias voltage. It simulates the device operating condition in an accelerated way in order to predict the long-term failure rate. High temperature storage life (HTSL) test is performed to assess the endurance of a device when exposed to a high temperature for a long time period. With the help of this test, thermally activated failure mechanisms of the semiconductor device can be exposed. The

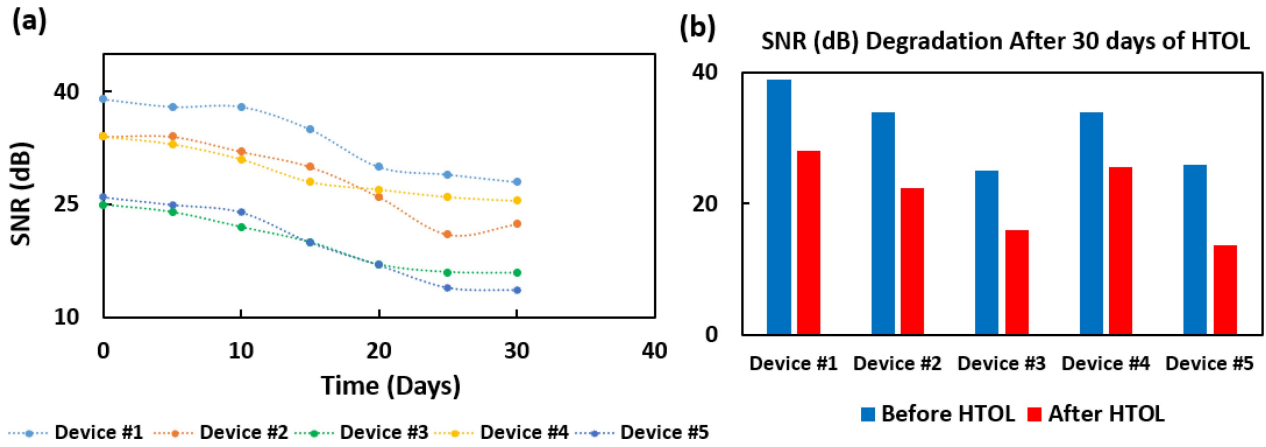


Fig. 3. (a) SNR responses of the sample ZnO/GaN devices for 500 ppm of ethanol in dry air at 20°C over 30 days due to HTOL test. (b) Comparison of SNR response of the devices before and after applying the HTOL stress for 30 days.

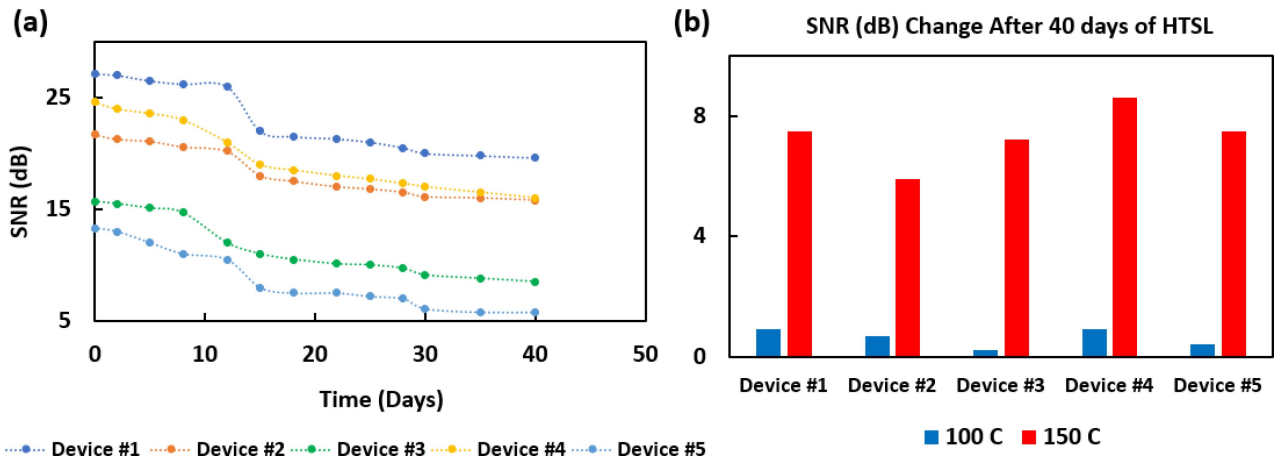


Fig. 4. (a) SNR responses of the sample ZnO/GaN devices for 500 ppm of ethanol in dry air at 20°C over 40 days of HTSL test. (b) Comparison of SNR changes of the sample devices at 100°C and 150°C of HTSL stress for 40 days.

purpose of temperature cycling test (TCT) is to evaluate the ability of the device to withstand both exposure to extreme temperatures and transitions between temperature extremes. This testing also exposes excessive thermal mismatch between materials. It can cause package cracking, passivation or metal de-lamination and cratering of the die, thus degrades electrical performance of the stressed device. Highly accelerated stress test (HAST) evaluates the reliability of non-hermetic packaged semiconductor devices in humid environments where temperature, humidity, and bias voltage accelerate the penetration of moisture. The trapped moisture facilitates electrolytic mechanism in presence of the applied bias, which causes metal corrosion and affects I-V characteristics of the device.

The main equipment used for these tests is a Tenny BTRC temperature and humidity test chamber. This chamber can simulate a wide range of temperature (-70°C to 200°C) and humidity conditions (10% to 95% of RH). The workspace within the chamber is fully insulated with a combination of fiberglass and polyurethane that optimizes the insulating characteristics of each material. Temperature and humidity set conditions are controlled by a bidirectional PID controller with a resolution of 0.1°C and 1% RH, respectively. Air heating is provided by electric heaters isolated from the workspace,

preventing direct radiation to the test device. The hermetic refrigeration system of the chamber operates on non-CFC refrigerants with LN_2 cooling boost.

IV. RESULTS AND DISCUSSION

From a batch of 50 fabricated devices, a sample population of 20 devices were taken for the accelerated stress tests (five devices for each test). Before applying the stress conditions, reference SNR responses of the sample ZnO/GaN devices have been recorded by exposing to 500 ppm of ethanol in dry air at room temperature (20°C). Then, the accelerated stress tests as mentioned in Table I have been performed on those sample devices and device responses have been measured at regular intervals. Catastrophic failure has not been observed in terms of gas sensing for the stressed devices except response degradation. Figure 3 shows the gradual SNR changes of the sensor devices due to HTOL test. It is observed that all devices are working with a maximum SNR degradation of 12.3 dB after applying the HTOL stress for 30 days. The fluctuation in SNR from sample to sample is attributed to the base-resistance fluctuation among sensor devices due to process variations. The difference in initial SNR does not impact on measured accelerated lifetimes and in turn predicted MTTF. Because, the failure

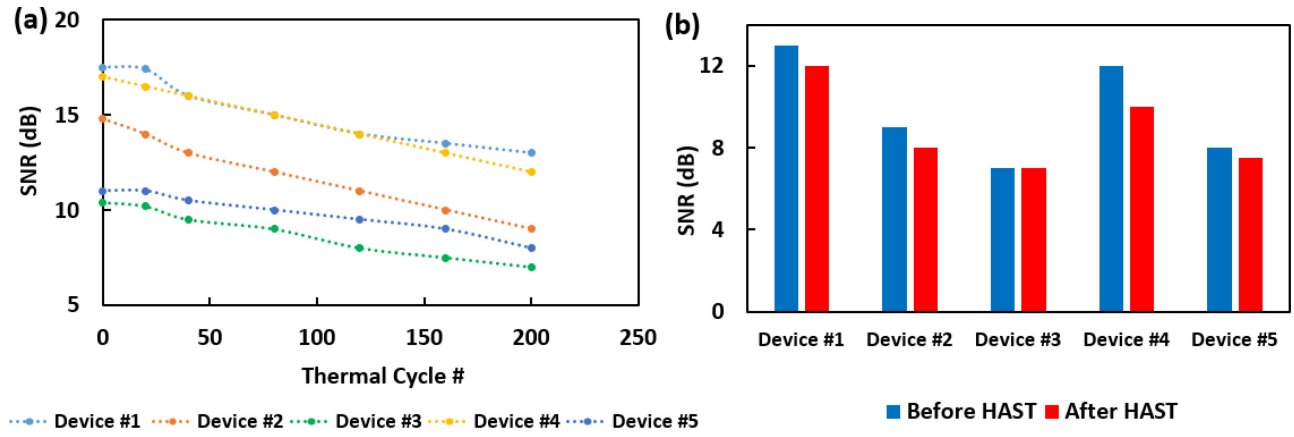


Fig. 5. (a) Variation of SNR responses of the ZnO/GaN devices with the number of thermal cycles applied in TCT test for 500 ppm of ethanol in dry air at 20°C. (b) Comparison of SNR of the ZnO/GaN devices before and after applying HAST stress.

TABLE II
ACCELERATED STRESS TESTS RESULTS SUMMARY AND FAILURE RATE CALCULATIONS

Accelerated Stress Test	Acceleration Factors	Stress time	Number of failures/Degree of freedom	χ^2 for 90% confidence level	Failure rate
HTOL	$AF_t = 18.9$ $AF_v = 4.8$	720 hrs	0/2	4.605	$2 \times 10^{-4} \text{ day}^{-1}$
HTSL	$AF_t = 30.2$	2400 hrs.	0/2	4.605	$7.6 \times 10^{-5} \text{ day}^{-1}$
TCT	$AF_{tc} = 8493$	500 cycles (dwell time=10 min, temp. transition time =15 min)	0/2	4.605	$1.3 \times 10^{-5} \text{ day}^{-1}$
HAST	$AF_t = 21.7$ $AF_h = 40$ $AF_v = 4.8$	96 hrs	0/2	4.605	$4.2 \times 10^{-4} \text{ day}^{-1}$

criteria are based on the percentage change of output SNR. Figure 4 illustrates the SNR degradations of the devices due to HTSL test. It is seen that all the sensors kept operating with a maximum SNR degradation of 8.6 dB at the end of 40 days of the HTSL stress. Figure 5(a) plots the change in device SNR with the number of thermal cycles applied in TCT test. It is found that metal lids of LCC packages came off for all test devices due to enduring abrupt temperature changes. However, all the stressed devices were still working fine with a maximum SNR degradation of 5.8 dB. The effect of the HAST experiment is presented in Figure 5(b). No failure mechanism has been observed on the device package due to the applied stress. All devices responses remain almost unaffected with a maximum SNR degradation of 2 dB. Therefore, the fabricated device materials are found robust against a continuous exposure to high humidity. The gradual degradation in ethanol exposure responses in all the stress tests is mainly attributed to the increase of sensor's base resistance and gradual phase transformation of receptor ZnO due to applied stresses [30]. All the accelerating factor calculations, test results and corresponding failure rate calculations using chi-square distribution are summarized in Table II.

By combining the failure rates (described in Section II) computed from the stress test results as presented in Table 2, total failure rate and lifetime of the device can be

estimated. Die/Process failure rate (λ_{die}) can be calculated as: $\lambda_{die} = \lambda_{HTSL} + \lambda_{HTOL} = 2 \times 10^{-4} + 7.6 \times 10^{-5} = 2.76 \times 10^{-4} \text{ day}^{-1}$. And, package failure rate ($\lambda_{package}$) can be calculated as: $\lambda_{package} = \lambda_{TCT} + \lambda_{UHAST} = 1.3 \times 10^{-5} + 4.2 \times 10^{-4} = 4.33 \times 10^{-4} \text{ day}^{-1}$. Therefore, total failure rate of devices (λ_{total}) can be predicted by combining the die and package failure rates, $\lambda_{total} = \lambda_{die} + \lambda_{package} = 7.09 \times 10^{-4} \text{ day}^{-1}$. Lifetime of the sensor device can be estimated by calculating mean-time-to-failure (MTTF) of the stressed devices using equations (7) and (8), where $MTTF = 1/\lambda_{total} = 3.87 \text{ years}$. Here, MTTF computation assumes a constant failure rate, meaning all the sensor devices have the same chance of failure when subjected to the same extreme environmental conditions. The estimation of device lifetime is largely influenced by the size of sample devices in stress tests and can be assumed minimum in this case. Taking a larger set of sample device would facilitate to obtain a longer statistical device lifetime.

V. CONCLUSION

Device reliability statistics is highly useful for predicting desired sensor performance over time and environmental conditions. In this study, two types of accelerated lifetime tests, sensor die test and device packaging reliability test, have been performed on ZnO/GaN nanowire-based sensor devices. The

JEDEC industrial standard accelerated stress tests, such as HTOL, HTSL, TCT and HAST, were conducted. The ethanol exposure responses from the stressed samples were recorded at regular intervals during the accelerated stress tests. No device failure was found in the performed stress tests except some minor packaging failure. However, ethanol sensing responses were degraded in terms of SNR with the increase of stress amount. Furthermore, estimation process of reliability indicators of the sensor device has been described. Statistical analysis was used to predict the failure rate and lifetime of the metal-oxide/GaN nanostructured sensor devices. The mean-time-to-failure (MTTF) of the stressed devices of this study is about 4 years.

ACKNOWLEDGMENT

The sensor devices were fabricated in the Nanofab of the NIST Center for Nanoscale Science and Technology. Stress tests and gas sensing measurements were conducted at N5 Sensors, Inc.

CONFLICTS OF INTEREST

There are no conflicts of interest to declare.

REFERENCES

- [1] J. Y. Tsao *et al.*, "Ultrawide-bandgap semiconductors: Research opportunities and challenges," *Adv. Electron. Mater.*, vol. 4, no. 1, Jan. 2018, Art. no. 1600501, doi: [10.1002/aelm.201600501](https://doi.org/10.1002/aelm.201600501).
- [2] A. Rani, K. DiCamillo, M. A. H. Khan, M. Paranjape, and M. E. Zaghloul, "Tuning the polarity of MoTe₂ FETs by varying the channel thickness for gas-sensing applications," *Sensors*, vol. 19, no. 11, p. 2551, Jun. 2019, doi: [10.3390/s19112551](https://doi.org/10.3390/s19112551).
- [3] G. S. Aluri *et al.*, "Highly selective GaN-nanowire/TiO₂-nanocluster hybrid sensors for detection of benzene and related environment pollutants," *Nanotechnology*, vol. 22, no. 29, Jul. 2011, p. 295503, doi: [10.1088/0957-4484/22/29/295503](https://doi.org/10.1088/0957-4484/22/29/295503).
- [4] T. Anderson *et al.*, "Advances in hydrogen, carbon dioxide, and hydrocarbon gas sensor technology using GaN and ZnO-based devices," *Sensors*, vol. 9, no. 6, pp. 4669–4694, 2009, doi: [10.3390/s90604669](https://doi.org/10.3390/s90604669).
- [5] G. Meneghesso *et al.*, "Reliability of GaN high-electron-mobility transistors: State of the art and perspectives," *IEEE Trans. Devices Mater. Rel.*, vol. 8, no. 2, pp. 332–343, Jun. 2008, doi: [10.1109/TDMR.2008.923743](https://doi.org/10.1109/TDMR.2008.923743).
- [6] G. S. Aluri *et al.*, "Methanol, ethanol and hydrogen sensing using metal oxide and metal (TiO₂–Pt) composite nanoclusters on GaN nanowires: A new route towards tailoring the selectivity of nanowire/nanocluster chemical sensors," *Nanotechnology*, vol. 23, no. 17, 2012, Art. no. 175501, doi: [10.1088/0957-4484/23/17/175501](https://doi.org/10.1088/0957-4484/23/17/175501).
- [7] G. S. Aluri, A. Motayed, A. V. Davydov, V. P. Oleshko, K. A. Bertness, and M. V. Rao, "Nitro-aromatic explosive sensing using GaN nanowire-titania nanocluster hybrids," *IEEE Sensors J.*, vol. 13, no. 5, pp. 1883–1888, May 2013, doi: [10.1109/JSEN.2013.2241423](https://doi.org/10.1109/JSEN.2013.2241423).
- [8] R. Bajpai *et al.*, "UV-assisted alcohol sensing using SnO₂ functionalized GaN nanowire devices," *Sens. Actuat. B, Chem.*, vols. 171–172, pp. 499–507, Aug./Sep. 2012, doi: [10.1016/j.snb.2012.05.018](https://doi.org/10.1016/j.snb.2012.05.018).
- [9] M. Khan, M. Rao, and Q. Li, "Recent advances in electrochemical sensors for detecting toxic gases: NO₂, SO₂ and H₂S," *Sensors*, vol. 19, no. 4, p. 905, Feb. 2019, doi: [10.3390/s19040905](https://doi.org/10.3390/s19040905).
- [10] M. A. H. Khan, B. Thomson, R. Debnath, A. Motayed, and M. V. Rao, "Nanowire-based sensor array for detection of cross-sensitive gases using PCA and machine learning algorithms," *IEEE Sensors J.*, vol. 20, no. 11, pp. 6020–6028, Jun. 2020, doi: [10.1109/JSEN.2020.2972542](https://doi.org/10.1109/JSEN.2020.2972542).
- [11] M. A. H. Khan and M. V. Rao, "Gallium nitride (GaN) nanostructures and their gas sensing properties: A review," *Sensors*, vol. 20, no. 14, p. 3889, Jul. 2020, doi: [10.3390/s20143889](https://doi.org/10.3390/s20143889).
- [12] *Search & Download JEDEC Documents*. Accessed: Jan. 15, 2020. [Online]. Available: <https://www.jedec.org/>
- [13] L. M. Klyatis, *Accelerated Reliability and Durability Testing Technology*. New York, NY, USA: Wiley, 2012.
- [14] *Toshiba Memory Corporation Reliability Handbook*, Toshiba Memory Corporation, Tokyo, Japan, 2018.
- [15] A. Viti, A. Terzi, and L. Bertolaccini, "A practical overview on probability distributions," *J. Thorac. Dis.*, vol. 7, no. 3, pp. E7–E10, Mar. 2015, doi: [10.3978/j.issn.2072-1439.2015.01.37](https://doi.org/10.3978/j.issn.2072-1439.2015.01.37).
- [16] *Analysis of On-going Environ. Stress Testing and Accelerated Reliability Testing of FUTEK Sensors*, FUTEK, Irvine, CA, USA, 2015.
- [17] *Quality and Reliability Manual*, ISSI, inc., Bengaluru, India, 2013.
- [18] L. A. Escobar and W. Q. Meeker, "A review of accelerated test models," *Stat. Sci.*, vol. 21, no. 4, pp. 552–577, 2006, doi: [10.1214/088342306000000321](https://doi.org/10.1214/088342306000000321).
- [19] *Semiconductor Reliability Handbook*, Renesas Electron., Koto City, Japan, 2017.
- [20] *Semiconductor Quality and Reliability Handbook: Chapter 2 Semiconductor Device Reliability Verification*, SONY, Minato City, Japan, 2013.
- [21] C. Shi *et al.*, "High-performance room-temperature TiO₂-functionalized GaN nanowire gas sensors," *Appl. Phys. Lett.*, vol. 115, no. 12, Sep. 2019, p. 121602, doi: [10.1063/1.5116677](https://doi.org/10.1063/1.5116677).
- [22] M. A. H. Khan, B. Thomson, J. Yu, R. Debnath, A. Motayed, and M. V. Rao, "Scalable metal oxide functionalized GaN nanowire for precise SO₂ detection," *Sens. Actuat. B, Chem.*, vol. 318, Sep. 2020, Art. no. 128223, doi: [10.1016/j.snb.2020.128223](https://doi.org/10.1016/j.snb.2020.128223).
- [23] M. A. H. Khan, B. Thomson, R. Debnath, A. Rani, A. Motayed, and M. V. Rao, "Reliable anatase-titania nanoclusters functionalized GaN sensor devices for UV assisted NO₂ gas-sensing in ppb level," *Nanotechnology*, vol. 31, no. 15, Apr. 2020, Art. no. 155504, doi: [10.1088/1361-6528/ab6685](https://doi.org/10.1088/1361-6528/ab6685).
- [24] M. A. H. Khan, B. Thomson, A. Motayed, Q. Li, and M. V. Rao, "Functionalization of GaN nanowire sensors with metal oxides: An experimental and DFT investigation," *IEEE Sensors J.*, vol. 20, no. 13, pp. 7138–7147, Jul. 2020, doi: [10.1109/JSEN.2020.2978221](https://doi.org/10.1109/JSEN.2020.2978221).
- [25] M. A. H. Khan, B. Thomson, A. Motayed, Q. Li, and M. V. Rao, "Metal-oxide/GaN based NO₂ gas detection at room temperature: An experimental and density functional theory investigation," in *Proc. Micro Nanotechnol. Sens. Syst. Appl. XII*, Apr. 2020, p. 103, doi: [10.1117/12.2557971](https://doi.org/10.1117/12.2557971).
- [26] J. P. Kozak, K. D. T. Ngo, D. DeVoto, and J. Major, *Impact of Accelerated Stress-Tests on SiC MOSFET Precursor Parameters*, document NREL/CP-5400-71331, Nat. Renew. Energy Lab., Golden, CO, USA, 2018.
- [27] *Quality & Reliability Handbook: Energy Efficient Innovations*, Phoenix, AZ, USA, On Semicond., 2018.
- [28] *Failure Mechanism Based Stress Test Qualification for Integrated Circuits: AEC - Q100 - Rev-H*, Autom. Electron. Council, 2014.
- [29] *JEDEC Standard, Reliability Qualification of Semiconductor Devices Based on Physics of Failure Risk and Opportunity Assessment*, JEDEC Standard JEP148A, Jan. 2014.
- [30] C. Wang, L. Yin, L. Zhang, D. Xiang, and R. Gao, "Metal oxide gas sensors: Sensitivity and influencing factors," *Sensors*, vol. 10, no. 3, pp. 2088–2106, Mar. 2010, doi: [10.3390/s100302088](https://doi.org/10.3390/s100302088).